P. Gallo, F. Berto,
Influence of surface roughness on high temperature fatigue strength and cracks initiation in 40CrMoV13.9 notched components,
Theoretical and Applied Fracture Mechanics,
Volume 80, Part B,
2015,
Pages 226-234,
ISSN 0167-8442,
https://doi.org/10.1016/j.tafmec.2015.07.003
https://www.sciencedirect.com/science/article/pii/S0167844215300392

Figures and tables are available at the bottom of the document.

Influence of surface roughness on high temperature fatigue strength and cracks initiation in 40CrMoV13.9 notched components

P. Gallo[1]*, F. Berto[1]

Department of Management and Engineering, University of Padova, Stradella San Nicola 3, 36100, Vicenza, Italy

**Corresponding author, email: pgallo@gest.unipd.it, berto@gest.unipd.it*

Abstract

The present paper addresses experimentally the high temperature fatigue of 40CrMoV13.9 steel and the effect of surface roughness on fatigue strength and cracks initiation.

The 40CrMoV13.9 steel considered here is widely used in different engineering high temperature applications among which hot-rolling of metals, where, in order to assure a constant temperature, the rolls are provided with cooling channels. These are the most stressed zone of the rolls where cracks initiate systematically.

In order to completely characterize the high temperature behaviour of this steel, firstly uniaxial-tension load controlled fatigue tests have been conducted at different temperatures up to 650°C. Two geometries are considered: plain specimens and plates weakened by symmetric V-notches, with opening angle and tip radius being equal to 90° and 1 mm, respectively. Subsequently, with the aim to investigate the influence of the cooling channels roughness on the high temperature behaviour and the cracks initiation, uniaxial-tension load controlled fatigue tests have been conducted on plate with central hole at the service temperature of 650°C, varying the surface roughness.

After a brief review of the recent literature, the experimental procedure is described in detail and the new data from un-notched and notched specimens are summarized in terms of stress range, at the considered temperatures.

Finally, fatigue data from un-notched and notched specimens are re-analysed by means of the mean value of the Strain Energy Density (SED) extended at high temperature.

Keywords. High temperature fatigue; Cracks growth; 40CrMoV13.9; Strain energy density; Surface roughness

1 Introduction

Hot-rolling process is increasingly required for higher mechanical performances, fatigue strength and quality of laminated products. Different steels have been employed in a large variety of applications to combine static and fatigue properties with an excellent wear resistance at high temperature and in corrosive environments. The 40CrMoV13.9 steel is widely used in different engineering high temperature applications among which hot-rolling of metals. Rolls for hot-rolling, despite different decisions made by different engineers in the design phase, have some basic characteristics, such as the presence of cooling channels with the aim to assure a uniform and controlled temperature during the in-service operations. On the basis of numerous direct feedbacks, the cooling channels are the most stressed zone of the rolls and cracks initiate systematically from this area. For these reasons, it becomes very interesting to deeply investigate this kind of steel, with the aim to completely characterize its fatigue behaviour at high temperature, considering for example notch effects and/or the influence of surface roughness on the crack initiation. These topics, especially if considering notched components at high temperature and high number of cycles are often ignored by the modern literature. However, it is possible to find some interesting works briefly reported hereafter.

Dealing with un-notched specimens, the fatigue behavior of different materials at high temperature has been investigated by some researchers such as [1–3]. In [1] an experimental investigation was conducted on 22Cr-20Ni-18Co-Fe alloy at elevated temperature using plain specimens. Fatigue tests were carried out at a constant temperature (871°C) while the strain ranged from 0.265 to 1.5 %. The fatigue lives varied from 10^3 to 10^6 cycles to failure. Cyclic deformation properties of the tested material were obtained from the tests and three fatigue models were applied discussing the advantages and drawbacks of each model. The fatigue properties and crack growth mechanism of a 2.25Cr–1Mo steel were investigated in [2]. The study was aimed to investigate the fatigue life up to 10^7 cycles of structural components used in hot and high-pressure environments. The tests were conducted on un-notched specimens in a temperature range varying between 20 and 500°C. The high-cycle fatigue life was found to be strongly influenced by the density and size of interior inclusions.

Dealing with 1.25Cr0.5Mo steel, high-temperature stress controlled tests were carried out at different loading conditions to investigate the fatigue–creep interaction behavior at high temperatures [3]. Four fatigue–creep facture maps were obtained showing that for stress amplitudes lower than the mean stress a close interaction between fatigue and creep occurred. This interaction provoked a visible reduction of the fatigue strength. The complex relationship between the fatigue life and the main influencing factors was explained by means of the strain rate at half-life, which was considered as the governing factor associated with the fatigue strength.

The increasing working temperature range and the growing necessity for greater efficiency and reliability of automotive exhaust system has been requiring the accurate investigation of the fatigue properties of heat resisting stainless steels at high temperature. Fully reversed axial fatigue tests were performed in [4] on smooth specimens of 18Cr–2Mo ferritic stainless steel (type 444) at room temperature, 673 K and 773 K in laboratory air, with the aim to investigate the effect of temperature on high cycle fatigue behavior. A notable influence of temperature on the fatigue strength was observed during the tests. The crack growth was found to be considerably faster at elevated temperatures than at room temperature and some fractographic analyses revealed brittle features in fracture surfaces near the crack initiation site, which were more pronounced and extensive at 773 K. An evident embrittlement occurred in the investigated temperature range and such embrittlement was found to be the main responsible for the observed decrease in the fatigue properties.

Dealing with non-ferrous materials, the effect of surface treatment on the stress/life fatigue behavior of a titanium Ti–6Al–4V turbine fan blade alloy has been recently investigated in the regime of 10^2–10^6 cycles to failure under fully reversed load-controlled isothermal push–pull loading, between 25°C and 550°C at a frequency of 5 Hz [5]. The fatigue behavior has been examined in plain specimens in the deep-rolled and laser-shock peened surface conditions, and compared to results on samples in the untreated (machined and stress annealed) condition. Although the fatigue resistance of the Ti–6Al–4V alloy declined with increasing test temperature regardless of surface condition, deep-rolling and laser-shock peening surface treatments were found to extend the fatigue lives by factors of more than 30 and 5–10, respectively, in the high-cycle and low-cycle fatigue regimes at temperatures as high as than 550 °C.

While results from un-notched materials are not so rare in the past and recent literature as just discussed, only few systematic investigations have been performed on notched specimens under fatigue loading at high temperature at medium-high cycle fatigue [6–8].

In [6,7], the notched fatigue strength of the nickel-base superalloy Inconel 718 was investigated under rotating bending loading at room temperature and 500°C in air. The linear notch mechanics was employed to assess the fatigue strength at elevated temperature being for that material the small-scale yielding conditions satisfied also at elevated temperature.

The effect of notch types and stress concentration factors on low cycle fatigue life and cracking of the DZ125 directionally solidified superalloy was experimentally investigated by Shi et al. [9]. Single-edge notched specimens with V and U type geometries were tested at 850 °C with a stress ratio R =0.01. The results revealed that the fatigue strength decreased with the elastic stress concentration factor, K_t, increasing from 1.76 to 4.35. The main conclusion of the paper was that K_t can be considered as a key parameter controlling the notch fatigue at least when the absolute dimensions of the tested notched specimens are similar.

In some recent contributions, the present authors have summarized the results from uniaxial tension load-controlled fatigue tests performed at high temperature on different materials [10–12]. Berto et al. [10] investigated the high temperature fatigue up to 650°C of Cu-Be specimens. Two geometries have been considered: hourglass-shaped specimens and plates weakened by a central hole. All fatigue data from un-notched and notched specimens have been reanalyzed there in terms of the mean value of the strain energy density evaluated, for the notched specimens, over a finite size control volume surrounding the highly stressed zone at the hole edge. This has permitted to summarize all fatigue data in a quite narrow scatter band. Gallo et al. [11] presented data from uniaxial-load controlled fatigue tests on notched specimens made of titanium Grade 2 at 500°C. Two geometries were considered: semicircular notches and plates weakened by lateral symmetric V-notches. Also in this case, the fatigue data from un-notched and notched specimens have been reanalyzed there in terms of the mean value of the strain energy density evaluated over a finite size control volume surrounding the notches. This has permitted to summarize all fatigue data in a quite narrow scatter band, regardless of the specimens geometries. Other authors has recently extended linear elastic approaches to assess high temperature fatigue such as Louks and Susmel [13] that investigated the accuracy of the linear-elastic Theory of Critical Distances (TCD) in estimating high-cycle fatigue strength of notched metallic materials experiencing elevated temperatures during in-service operations, with very good results.

The number of paper remains very poor if considering works on the influence of the surface roughness on the fatigue behavior at high temperature. However it is a very interesting topic from industrial viewpoint since the investigation of the cooling channels roughness on the high temperature behaviour and the cracks initiation can lead to several advantages: first of all, it defines quantitatively the influence of the surface roughness on the fatigue performances, and therefore justifies the costs to obtain a high surface finish quality. This makes possible to evaluate in terms of cost-benefit analysis the choice of imposing a law surface roughness or, otherwise, high surface roughness.

An interesting work is presented by [14] on the sensitivity of surface crack initiation to surface roughness in LCF at 550 °C of AISI 404L and Cr-Mo-V steel, in a pure argon atmosphere, also under creep-fatigue interaction condition. The creep-fatigue interaction was obtained by the introduction of tensile hold time. Two different states of surface finish were obtained by mechanical polishing with emery papers of grade nos. 80 and 1200 respectively. For Cr-Mo-V steel specimens, the maximum value for the depth of the surface polished with emery paper nos. 80 and 1200 are about 8.0 and 0.4 μm respectively. The result of the tests shown that for Cr-Mo-V steel the fatigue life of the specimen polished with emery paper no. 80 is significantly reduced (about 50%) compared with that of the specimen polished with emery paper no. 1200. The same trend was registered independent of the creep-fatigue interaction condition, that is a very important consideration. Since the surface roughness affects only the surfacial phenomena like crack initiation, they concluded that the number of cycles for crack initiation was a large fraction of the fatigue life, both in the case of pure fatigue or fatigue-creep interaction. This is a very important conclusion because supports the significance to investigate the influence of the surface roughness on the crack initiation since this phase is the one that involves a large fraction of fatigue life. Moreover they observed that no grain boundary cavitation was detected during the tests and the fracture mode was observed to be transgranular. For such material, where transgranular crack initiation is faster in the specimen with a rough surface than in that with a smooth surface, the surface roughness has a strong influence on the creep-fatigue and pure fatigue life. The results were in agreement with a previous work by the same author [15] considering only Cr-Mo-V steel. In that work they tested cylindrical specimens made of Cr-Mo-V steel at 550 °C. Two different modes of surface roughness were obtained by mechanically polishing specimens with emery paper nos. 80 and 1200. They showed that a large fraction of the fatigue life is consumed in the crack initiation and that the effect of surface roughness on low-cycle fatigue life could be due to the reduction of the number of cycles for crack initiation.

In the above background, the present work deals with high temperature fatigue tests of 40CrMoV13.9. The tested material is characterized by four different heat treatments able to assure a high strength at room and elevated temperatures. The most important application is cold or hot rolling of metals. A complete set of data from notch specimens under torsion and combined tension and torsion loadings at room temperature has been recently provided by the present authors [16].

At the best of authors' knowledge, a complete set of data from un-notched and notched specimens at high temperature, as a complete characterization on the influence of the surface roughness, is not available in the literature for 40CrMoV13.9. With the aim to fill this lack, the present paper experimentally investigate the high temperature fatigue of notched components of the considered alloy at different temperatures up to 650°C. Subsequently, with the aim to investigate the influence of the rolls cooling channels roughness on the high temperature behaviour and the cracks initiation, fatigue tests have been conducted on plate with central hole at the service temperature of 650°C.

The final objective of this study is to present a set of new results from high-temperature fatigue tests on 40CrMoV13.9 un-notched and notched specimens in the medium- and high-cycle regime (10^5–10^6 cycles). All the tests have been performed under uniaxial tension and load controlled conditions.

A final synthesis of the present results together with previous data from multiaxial tests (at room temperature) on the same material [16] is carried out by means of the Strain Energy Density (SED) approach, as recently made for Cu-Be alloys [10] and Titanium Grade 2 [11], at elevated temperature.

2 Experimental details

2.1 Material

The material investigated in the present study is 40CrMoV13.9 steel, usually employed for hot-rolling of metals where the material is subjected to a combination of mechanical and thermal loading conditions. Preliminary static tensile tests on a standard specimen were carried out to evaluate the elastic and strength properties at 650°C: Young's modulus E is equal to 135 GPa, σ_Y is equal to 520 MPa and σ_R to 610 MPa. The data-sheet reports the following mechanical properties at room temperature (25°C): elastic modulus E is equal to 206 GPa, tensile strength of about 1300 MPa and a yield strength of 1100 MPa with a percent elongation of 15%. The properties (at room temperature and 650°C) are also summarized in Table 1.

The chemical composition of the material and the heat treatment schedule are given in Table 2 and Table 3, respectively. The material was first quenched at 920°C and subsequently tempered twice at 580°C and 590°C. A final stress relieving treatment at 570°C was carried out. The final microstructure was characterized by a high strength bainitic-martensitic structure. The microstructure of the specimens is shown in Fig. 1 at different magnification values. It is evident that the microstructure is homogenous along all the directions, also through the specimen thickness, due to the austenitizing and annealing processes.

2.2 Specimen geometry

Considering the high temperature fatigue tests and the investigation of the cracks growth, three specimen geometries were considered:

- Hourglass shaped (smooth) specimens with a theoretical stress concentration factor close to 1.0 (see Figure 2);
- Plates weakened by lateral symmetric V-notches, with a net cross section of 20 mm × 5 mm and a total length of 300 mm (Figure 3). The notches were characterized by a depth, *a*, equal to 5 mm, an opening angle, 2α, equal to 90° and a notch tip radius ρ=1 mm. This geometry results in a theoretical stress concentration factor $K_{t,n}$=3.84 (on the net transverse sectional area).
- Plates with a central hole (see Figure 4), with a cross section of 30 mm x 5 mm and a total length of 300 mm; the hole radius is 10 mm, which results in a theoretical stress concentration factor $K_{t,n}$ = 2.3 (on the net transverse area).

The specimens were designed to avoid an increase of temperature near the grippers and the length of 300 mm, which is higher than the length usually adopted at room temperature, was chosen for this reason. The diameter of the hole, instead, matches the real dimension of the rolls cooling channels.

2.3 Fatigue equipment and testing procedures

The fatigue tests are conducted on a servo-hydraulic MTS 810 test system with a load cell capacity of 250 kN. The system is provided with a MTS Model 653 High Temperature Furnace. It is ideal for a wide variety of high-temperature tests, including tension, compression, bending and fatigue testing of different materials, metallic and not. It has a center-split design that enables easy access to both grippers and specimens. The furnace includes the MTS digital PID Temperature Control System and is configured for two heating zones which can be independently temperature-controlled through high precision thermocouples. The zone at constant temperature is 80 mm length. The heating elements are made of silicon carbide. An insulation plate situated between the upper and lower elements helps to ensure reliable zone separation and pre-cut insulation reduces heat loss. This furnace is particularly well-suited for applications that require a lower thermal gradient on a fatigue (or tensile) specimen. The nominal temperature for this furnace ranges from 100°C to 1400°C and the control point stability is about ± 1°C. Since the wedge grips are affected by the heat of the furnace, they are equipped with a cooling system that keeps the temperature low enough in order to not provoke any damage to the test-instruments.

In order to completely characterize the high temperature behavior of the considered alloy, firstly load-controlled fatigue tests were carried out at different temperatures. More precisely, the hour-glass shaped specimens were tested at room temperature, 360°C and 650°C; the V-notched specimens were tested at room temperature, 360°C, 500°C and 650°C. Overall, eight fatigue curves were obtained by testing more than 60 specimens. The specimen was heated to reach the desired temperature and after a short waiting period (10 minutes) necessary to assure a uniform temperature, the test was started. The temperature was maintained constant until specimen failures thank to the PID temperature control system. The uniaxial tensile fatigue tests were carried out over a range of cyclic stresses at the constant frequency of 5 Hz; the nominal load ratio R was kept constant and equal to 0.01.

Regarding, instead, the investigation on the influence of the surface roughness on the crack initiation, the plates with central hole were tested only at the service temperature of 650°C. The specimen was heated to reach the desired temperature, and after a short waiting period necessary to assure a uniform temperature, the test was started. Because of the available equipment, it was not possible to monitor continuously, in real time, the specimen hole. For this reason, an alternative procedure has been adopted for the cracks detection: once reached a specific number of cycles, the test was temporarily stopped and the specimen checked through an optical microscope with the aim to detect any sign of cracks initiation. This operation was repeated until the crack was detected. The intervals, at which the tests were paused, were smaller as the number of cycles increasing (e.g. defining intervals 2500 N length, where necessary). After some calibration trials, a good reliable procedure was defined, especially for high number of cycles (i.e. for low loads) that are the most interesting for the final applications. The values of the stiffness, registered in real-time by the machine, also helped to define the procedure and the crack detection: the experimental evidences shown a significant drop of the stiffness as one or more cracks initiated. For this reason, that variable was very useful as a kind of warning that something was happened. Once detected stiffness variation, in fact, systematically after a few number of cycles (about 10000 to 30000 cycles) a crack appeared visible at the optical microscope. So the visual detection helped to define a good number of cycles range at which the crack initiated, while the stiffness variation defined a more accurate number of cycles within that range, a posteriori (analyzing the stored data), usually smaller than that of the optical detection.

The uniaxial tensile fatigue tests were carried out over a range of cyclic stresses at the constant frequency of 5 Hz while the nominal load ratio R was kept constant and equal to 0.01. The following values of the surface roughness, as the arithmetic average of the roughness profile, were considered for the plates with central hole: 2µm, 1µm, 0.4µm, 0.15µm.

3 Results

3.1 Fatigue curves

The fatigue data were statistically re-analyzed by using a log-normal distribution and are plotted in terms of nominal stress ranges (referred to the net area) in Figures 5 and 6. More specifically, Figure 5 shows the fatigue data of the hourglass specimens, the Wöhler curve (mean curve, P_s = 50%), the Haibach scatter band referred to 10% and 90% probabilities of survival (for a confidence level equal to 95%) and the inverse slope k of the curves. Data from specimens tested at room temperature and at T=360°C are found to belong to the same scatterband, with a value of the scatter index quite low, T_σ=1.29. The scatter of the specimens tested at T=650°, instead, is higher being T_σ=2.00, which show also a strong decrease of the fatigue strength combined with a strong variation of the slope. A vertical line is drawn in correspondence of one million cycles where the mean values of the stress range are given to make the comparison easier. At 10^6 cycles the stress range is equal to 675.14 MPa when T≤360°C, while it is equal to 95.23 MPa at 650°C.

Fatigue data of the specimens weakened by lateral V-notches are shown in Figure 6 at different temperatures. The run-out specimens (marked by tilted arrow) were excluded from the statistical analysis. It is evident that up to 500°C there are no differences with respect to the room temperature, whereas a substantial decrease of fatigue strength can be observed at 650°C. The scatter-band related to the specimens tested at T=650°C is compared with that summarizing data obtained for T≤500°C. At one million cycles, the value of the stress referred to a probability of survival of 50% decreases from 213.12 to 74.32 MPa. The variation of the slope is also strong, it decreases from k=5.14 to k=2.91. Conversely, the values of the scatter index are comparable.

For the sake of completeness, the results are also summarized in details in Table 4.

The drastic decrease of the fatigue properties observed at 650°C is linked to the specific heat treatments made on the material. The maximum temperature in the tempering treatment was equal to 590°C and the last stress relieving treatment was carried out at 570°C. Experimental data clearly document that under long time exposure at temperatures higher than 570-590°C all beneficial effects due to the heat treatments are lost.

By comparing the reduction of the fatigue strength exhibited at 10^6 cycles by the notched specimens tested at room temperature with respect to un-notched ones, one determines a fatigue strength reduction factor K_f equal to 3.17, which is a little lower than the theoretical stress concentration factor $K_{t,n}$=3.84 obtained by means of a FE analysis (Ansys code) and in good agreement with the value provided by

Peterson's handbook. This means that a notch root radius ρ=1 mm involves the notch sensitivity index is less than 1.0. It is worth noticing that the fatigue strength reduction factor K_f at 650°C is equal to 1.48, which is remarkably lower than the value determined at room temperature. It is evident that the high temperature has strongly reduced the notch sensitivity of the steel.

3.2 Influence of surface roughness on high temperature fatigue and crack initiation

The 40CrMoV13.9 steel is widely used in different engineering high temperature applications among which hot-rolling of metals, where, in order to assure a constant temperature, the rolls are provided with cooling channels. These are the most stressed zone of the rolls where cracks initiate systematically. The surface roughness is one of few parameters that can be set in the design stage. With the aim to investigate the influence of the cooling channels roughness on the high temperature behaviour and the cracks initiation, uniaxial-tension load controlled fatigue tests have been conducted on plate with central hole at the service temperature of 650°C, as reported some sections above.

The understanding of the influence of this parameter on the component performances can lead to several advantages: first of all, it defines quantitatively the influence of the surface roughness on the fatigue performances, and therefore justifies the relative costs in order to obtain a high surface finish quality. This makes possible to evaluate in terms of cost-benefit analysis the choice of imposing a law surface roughness or, otherwise, high surface roughness.

The obtained Wöhler curves (mean curve, P_s = 50%) are summarized in Figure 7, in terms of stress range (referred to the net area). A vertical line is drawn in correspondence of two million cycles and one million cycles. The run-out specimens were not considered in the statistical analysis and are marked with a tilted arrow. From the figure it is clear how the roughness influences the fatigue strength. For poor roughness, the effects on the fatigue behaviour are negligible. In fact, there are no differences between the curves regarding R_a=2µm and R_a=1µm, especially if considering the stress range at one million cycles (that is the most interesting for the final application). When the quality of the surface finish is improved, we can see some enhancements on the fatigue behaviour. The more evident improvement is registered for the value of R_a=0.15µm. Comparing this value with that of the starting poor roughness, the stress range at one million cycles increases of 44%, that is a very remarkable result, in agreement with [15]. Similar results for other materials have been obtained recently by other authors such as Hussain et al. [17], Gao et al. [18]: from these works also emerged that a good surface finishing has a beneficial effect on the fatigue limit, even if the effects were not notable in comparison with those of the present paper and [15].

The decrement of the fatigue life of the specimens with rough surfaces at high temperature suggests this result is originated from the reduction in the number of cycles for crack initiation. It can be asserted that a large number of fraction of the high temperature fatigue life was spent in the crack initiation process in agreement with [14,15].

In order to better support the conclusions, an analysis on the crack initiation near the hole has been conducted. The plates with central hole were tested at 650°C and once reached a specific number of cycles, the test was temporarily stopped and the specimen checked through an optical microscope with the aim to detect any sign of cracks initiation. Figure 8 depicts an example of the crack detection. The number of cycles to crack initiation and failure for a constant stress range as a function of the surface roughness is reported in Figure 9. The stress range is selected in order to analyse the high cycle fatigue life. Some considerations deserve to be spent on this figure: above all, it is clear the beneficial effect of the surface roughness on the fatigue behaviour, in fact for the same stress range of 240MPa, an R_a of 2μm returns an N_i equal approximately to 1E+05 cycles, that becomes almost 1E+06 for an R_a=0.15μm, a very remarkable results; secondly, the number of cycles for crack initiation is very near to the number of cycles to failure, supporting the thesis that a large number of fraction of the fatigue life was spent for the crack initiation phase. The ratio between N_i and N is always greater than 0.8, for all of the surface roughness values. On the basis of the experimental evidences, a good surface finish quality can be justified by the resultant beneficial effects.

4 A synthesis in terms of linear elastic SED of room and high temperature data

The new high temperature data from unnotched and V-notched specimens made of 40CrMoV13.9 are summarized in this section by using the SED approach. On the basis of the experimental evidences of the present work, the synthesis in terms of SED has been carried out up to 500°C considering the same critical radius used in Ref. [12] for multiaxial fatigue data. In fact, as visible from Figures 5 and 6, no reduction in the fatigue strength has been detected until 500°C both for unnotched and notched specimens.

In the medium and high cycle fatigue regime the critical SED range for un-notched specimens can be simply evaluated by using the following expression:

$$\Delta\overline{W} = \frac{c_w}{2E}\Delta\sigma_n^2 \qquad (1)$$

In Eq. (5) $\Delta\sigma_n$ is the nominal stress range referred to the net sectional area. As already said, the weighting parameter c_W has to be applied to take into account different values of the nominal load ratio[19]. Being the actual tests referred to R=0.01, c_w is equal to 1.0. Since Eq. (1) is applied at different temperatures, the Young's modulus has to be updated as a function of the temperature.

E is equal to 206 GPa at room temperature and 135 GPa at 650°C. The datasheet also provided the values of the Young modulus for the other temperatures: at 360°C the Young's modulus E results to be 165GPa and at 500°C it is equal to 150 GPa. These values have been obtained experimentally by the manufacturer, with the assistance of an external laboratory. It is possible to see that the Young modulus shows a linear trend as function of the temperature, which has been found also by other authors [20].

For the notched specimens Eq. (2) can be directly applied. For the specific case of 2α=90° and R_c/ρ=0.05, parameters F and H are equal to 0.7049 and 0.5627, respectively [21]. The stress concentration factor referred to the net area is equal to 3.84.

$$\Delta\overline{W} = c_w F(2\alpha) \times H(2\alpha, \frac{R_c}{\varrho}) \times \frac{K_{t,n}^2 \Delta\sigma_n^2}{E} \qquad (2)$$

Here $\Delta\sigma_n$ is the stress range, $K_{t,n}$ is the theoretical stress concentration factor (both referred to the net sectional area), E is the Young's modulus. F(2α) depends on the notch opening angle and is equal to 0.705 for 2α=90°. Finally H depends both on the notch angle and the critical radius-notch tip radius ratio.

By using Equations (1) and (2) the new data from the tests carried out at room temperature up to 500°C can be summarized in Figure 10 in a single narrow scatterband, characterized by an inverse slope k equal to 5.31 and a scatter index T_W equal to 2.25. Moreover, the new data belong to the same scatter-band of multiaxial room-temperature fatigue data taken from literature [16] and regarding the same material. Thanks to the SED approach it has been possible to summarize in a single scatterband all the fatigue data, independently of the specimen geometry, of the temperature (up to 500°C) and, considering the multiaxial data reported in [16] and in Fig. 10, also of the loading condition.

Dealing with data carried out at 650°C, the fatigue strength of unnotched and notched specimens has been found strongly lower than the corresponding data from tests carried out at T<500°C. For this specific temperature (T=650°), which is important in practical industrial applications, in particular for hot rolling of aluminum alloys, an empirical formula has been proposed for notched specimens by modifying Eq.(2). This allows us to take into account the notch sensitivity of this material at temperatures higher than 500°C:

$$\Delta\overline{W} = c_w Q(T) L(f/f_0) F(2\alpha) \times H(2\alpha, \frac{R_c}{\varrho}) \times \frac{K_{t,n}^2 \Delta\sigma_n^2}{E} \quad (3)$$

Q (T) is the notch sensitivity function at a specific temperature T. This function has to be set (as a function of the temperature T) by equating at high cycle fatigue (10^6 cycles) the SED value from plain specimens and those from notched specimens; f is the test frequency of notched specimens at high temperature and f_0 the test frequency of unnotched specimens at the same temperature. L is a function related to the sensitivity of the material to the load frequency and depends on the ratio f/f_0. Function L is required to be equal to 1.0 if $f=f_0$, a condition respected in all tests of the present analysis. The critical radius R_c is kept constant and equal to that obtained at room temperature (R_c=0.05 mm). Dealing with our specific case Q (T=650°C)= 0.18. Equation (3) can be re-written by substituting the numerical value of each function:

$$\Delta\overline{W} = 1.0 \times 0.18 \times 1.0 \times 0.7049 \times 0.5627 \frac{K_{t,n}^2 \Delta\sigma_n^2}{E} = 0.07139 \frac{K_{t,n}^2 \Delta\sigma_n^2}{E} \quad (4)$$

Where, as said above, $K_{t,n}$=3.84.

Considering Eq. (4) applied to notched specimens and Eq. (1) applied to plain specimens, the SED master curve for 40CrMoV13.9 at 650°C has been obtained. The fatigue data from tests at 650°C are plotted in terms of averaged strain energy density range over a control volume in Figure 11, considering the critical radius previously derived at room temperature. It is possible to observe that the scatter band is quite narrow, with the scatter index being T_W = 2.56 that results in T_σ=1.60 in terms of equivalent local stress range. The inverse slope of the scatterband is equal to 1.43. Thanks to the SED approach it is possible to summarise in a single scatterband all the fatigue data at the same temperature, regardless of the specimen geometry.

Future developments will be devoted to set the proposed empirical equation to other geometries and temperatures. The idea is to further increase the temperature, in order to study the interactions between fatigue and creep. Another open point is the behaviour of the same steel under different loading conditions, for example in prevalent mode II or in combined mode I and mode III loading conditions.

Another important aspect worth investigating is the constraint effect through the plate thickness. It can play a fundamental role in fracture and fatigue assessment.

Conclusion

The present paper addresses experimentally the high temperature fatigue of 40CrMoV13.9 steel and the effect of surface roughness on fatigue strength and cracks initiation. In order to completely characterize the high temperature behaviour of this steel, firstly uniaxial-tension load controlled fatigue tests have been conducted at different temperatures up to 650°C. Two geometries are considered in this phase: plain specimens and plates weakened by symmetric V-notches, with opening angle and tip radius being equal to 90 degrees and 1 mm, respectively. Subsequently, with the aim to investigate the influence of the roughness on the high temperature behaviour and the cracks initiation, uniaxial-tension load controlled fatigue tests have been conducted on plate with central hole at the service temperature of 650°C. This geometry simulates the cooling channels of rolls for hot-rolling of metals, which are the most stressed zone of the rolls. The understanding of the influence of the surface finish on the component performances can lead to several advantages from industrial viewpoint. Moreover, the work has been motivated by the fact that, at the best of authors' knowledge, only a limited number of works dealing with high-temperature fatigue are available in the literature and no results seem to be available from notched components made of this steel tested at elevated temperatures.

Finally, fatigue data from un-notched and notched specimens are re-analysed by means of the mean value of the Strain Energy Density (SED) extended at high temperature.

The main results can be summarized as follows:

- The tested alloy exhibits good high temperature fatigue behaviour up to 500°. Until that temperature, no reduction in the fatigue strength with respect to the room temperature has been detected for plain and V-notched specimens. Above 500°C, instead, a significant reduction in fatigue strength is shown (see Figure 5 and Figure 6).
- At 650°C the notch sensitivity of the present steel seems to be quite low. The inverse slope k is also very similar. It is equal to 2.48 for hourglass shaped specimens and 2.91 for plates weakened by lateral notches.

- The strong reduction of the fatigue properties of the present material at 650°C can be attributed to the specific thermal treatments performed on it. In fact the material was first quenched at 920°C and subsequently tempered at about 580°C twice. A final stress relieving treatment at 570°C was carried out. The tempered temperature and final stress relieving temperatures were lower than 650°C. It seems that for a long time exposure at temperatures higher than 570-590°C the beneficial effects due to these specific treatments were lost.

- All new data from tests carried at room temperature up to 500°C are summarized in terms of mean SED over a control volume with R_c=0.05 mm. A sound agreement in terms of SED has been found between the present results and those recently obtained from a large bulk of multiaxial tests performed at room temperature on the same material.

- A quite narrow scatter band characterized by a limited value of the scatter index has been obtained by summarizing together new data and old multiaxial data taken by [12] up to 500°C.

- A specific master curve based on SED has been proposed for the considered steel tested at T=650°C in Fig 11. The scatter band makes possible to summarize together data from plain and notched specimens. Dealing with notched specimens an empirical expression has been also proposed for the SED calculation. The equation can be directly employed for practical applications of 40CrMoV13.9 steel at 650°C.

- The roughness influences the fatigue strength. When the quality of the surface finish is improved, we can see some enhancements on the fatigue behaviour. The more evident improvement is registered for the value of R_a=0.15μm. Comparing this value with that of the starting poor roughness, the stress range at one million cycles increases of 44%. These results are well supported by Fig. 7.

- The decrement of the fatigue life of the specimens with rough surfaces at high temperature suggests this result is originated from the reduction in the number of cycles for crack initiation and it is clear the beneficial effect of the surface roughness on the fatigue behaviour. In fact for the same stress range of 240MPa, an R_a of 2μm returns an N_i equal approximately to 1E+05 cycles, that becomes almost 1E+06 for an R_a=0.15μm as shown in Fig. 7.

- The ratio between N_i (number of cycles to crack initiation) and N (number of cycles to failure) is always greater than 0.8, for all of the surface roughness values (see Fig. 9), proving that a large fraction of the fatigue life is spent for crack initiation phase.

References

[1] T.H. Krukemyer, A. Fatemi, R.W. Swindeman, Fatigue Behavior of a 22Cr-20Ni-18Co-Fe Alloy at Elevated Temperatures, J. Eng. Mater. Technol. 116 (1994) 54.

[2] H. Kobayashi, a Todoroki, T. Oomura, T. Sano, T. Takehana, Ultra-high-cycle fatigue properties and fracture mechanism of modified 2.25Cr–1Mo steel at elevated temperatures, Int. J. Fatigue. 28 (2006) 1633–1639.

[3] Z. Fan, X. Chen, L. Chen, J. Jiang, Fatigue–creep behavior of 1.25Cr0.5Mo steel at high temperature and its life prediction, Int. J. Fatigue. 29 (2007) 1174–1183.

[4] Y. Uematsu, M. Akita, M. Nakajima, K. Tokaji, Effect of temperature on high cycle fatigue behaviour in 18Cr–2Mo ferritic stainless steel, Int. J. Fatigue. 30 (2008) 642–648.

[5] I. Altenberger, R.K. Nalla, Y. Sano, L. Wagner, R.O. Ritchie, On the effect of deep-rolling and laser-peening on the stress-controlled low- and high-cycle fatigue behavior of Ti–6Al–4V at elevated temperatures up to 550°C, Int. J. Fatigue. 44 (2012) 292–302.

[6] Q. Chen, N. Kawagoishi, H. Nisitani, Evaluation of notched fatigue strength at elevated temperature by linear notch mechanics, Int. J. Fatigue. 21 (1999) 925–931.

[7] N. Kawagoishi, Q. Chen, H. Nisitani, Fatigue strength of Inconel 718 at elevated temperatures, Fatigue Fract. Eng. Mater. Struct. 23 (2000) 209–216.

[8] F. Berto, P. Gallo, P. Lazzarin, High Temperature Fatigue Tests of a Cu-Be Alloy and Synthesis in Terms of Linear Elastic Strain Energy Density, Key Eng. Mater. 627 (2014) 77–80.

[9] D.Q. Shi, X.A. Hu, J.K. Wang, H.C. Yu, X.G. Yang, J. Huang, Effect of notch on fatigue behaviour of a directionally solidi fi ed superalloy at high temperature, (2013) 1288–1297.

[10] F. Berto, P. Lazzarin, P. Gallo, High-temperature fatigue strength of a copper-cobalt-beryllium alloy, J. Strain Anal. Eng. Des. 49 (2014) 244–256.

[11] P. Gallo, F. Berto, P. Lazzarin, High temperature fatigue tests of notched specimens made of titanium Grade 2, Theor. Appl. Fract. Mech. 76 (2015) 27–34.

[12] F. Berto, P. Lazzarin, C. Marangon, Fatigue strength of notched specimens made of 40CrMoV13.9 under multiaxial loading, Mater. Des. 54 (2014) 57–66.

[13] R. Louks, L. Susmel, The linear-elastic Theory of Critical Distances to estimate high-cycle fatigue strength of notched metallic materials at elevated temperatures, Fatigue Fract. Eng. Mater. Struct. (2014) In press.

[14] J.J. Kim, S.W. Nam, J.H. Ryu, The sensitivity of surface crack initiation to surface roughness in low-cycle fatigue at high temperature, Mater. Sci. Eng. A. 130 (1990) L7–L10.

[15] J. Ryu, S. Nam, Effect of surface roughness on low-cycle fatigue life of Cr-Mo-V steel at 550 °C, Int. J. Fatigue. 11 (1989) 433–436.

[16] F. Berto, P. Lazzarin, C. Marangon, Fatigue strength of notched specimens made of 40CrMoV13.9 under multiaxial loading, Mater. Des. 54 (2014) 57–66.

[17] K. Hussain, D.S. Wilkinson, J.D. Embury, Effect of surface finish on high temperature fatigue of a nickel based super alloy, Int. J. Fatigue. 31 (2009) 743–750.

[18] Y.K. Gao, X. Bin Li, Q.X. Yang, M. Yao, Influence of surface integrity on fatigue strength of 40CrNi2Si2MoVA steel, Mater. Lett. 61 (2007) 466–469.

[19] P. Lazzarin, C.M. Sonsino, R. Zambardi, A notch stress intensity approach to assess the multiaxial fatigue strength of welded tube-to-flange joints subjected to combined loadings, Fatigue Fract. Eng. Mater. Struct. 27 (2004) 127–140.

[20] B.A. Latella, S.R. Humphries, Young's modulus of a 2.25Cr–1Mo steel at elevated temperature, Scr. Mater. 51 (2004) 635–639.

[21] P. Lazzarin, F. Berto, Some Expressions for the Strain Energy in a Finite Volume Surrounding the Root of Blunt V-notches, Int. J. Fract. 135 (2005) 161–185.

Temperature	E (GPa)	σ_R (MPa)	σ_Y (MPa)	Elongation to fracture (%)	HRC
Room Temp.	206	1355	1127	15.2	52
650°C	135	610	520	23.5	35

Table 1: Mechanical properties of 40CrMoV13.9.

C	Mn	Si	S	P	Cr	Ni	Mo	V	Al	W
0.38	0.5	0.27	0.006	0.003	3.05	0.24	1.04	0.24	0.013	0.005

Table 2: Chemical composition wt.%, balance Fe.

	Heat treatment	Heating ratio (°C/h)	Temperature (°C)	Holding (hours)	Cooling
1	Quenching	100	920 ± 10	3	water
2	Tempering 1	100	580 ± 10	5	air
3	Tempering 2	100	590 ± 10	5	air
4	Stress relieving	100	570 ± 10	3	air

Table 3: Thermal treatment of the considered material

Specimen - T (°C)	k	T_σ	σ_{max}(10^6 cycles)		
			10% (MPa)	50% (MPa)	90% (MPa)
HG - room to 360°C	7.28	1.29	766	675	595
HG - 650°C	2.48	2.00	124	95	67
V- room to 500°C	5.14	1.48	259	213	174
V - 650°C	2.91	1.63	94	74	58

Table 4: Results from fatigue tests at different temperatures. Stresses referred to the net area. HG stands for hour-glass shaped specimens while V stands for V-notched ones.

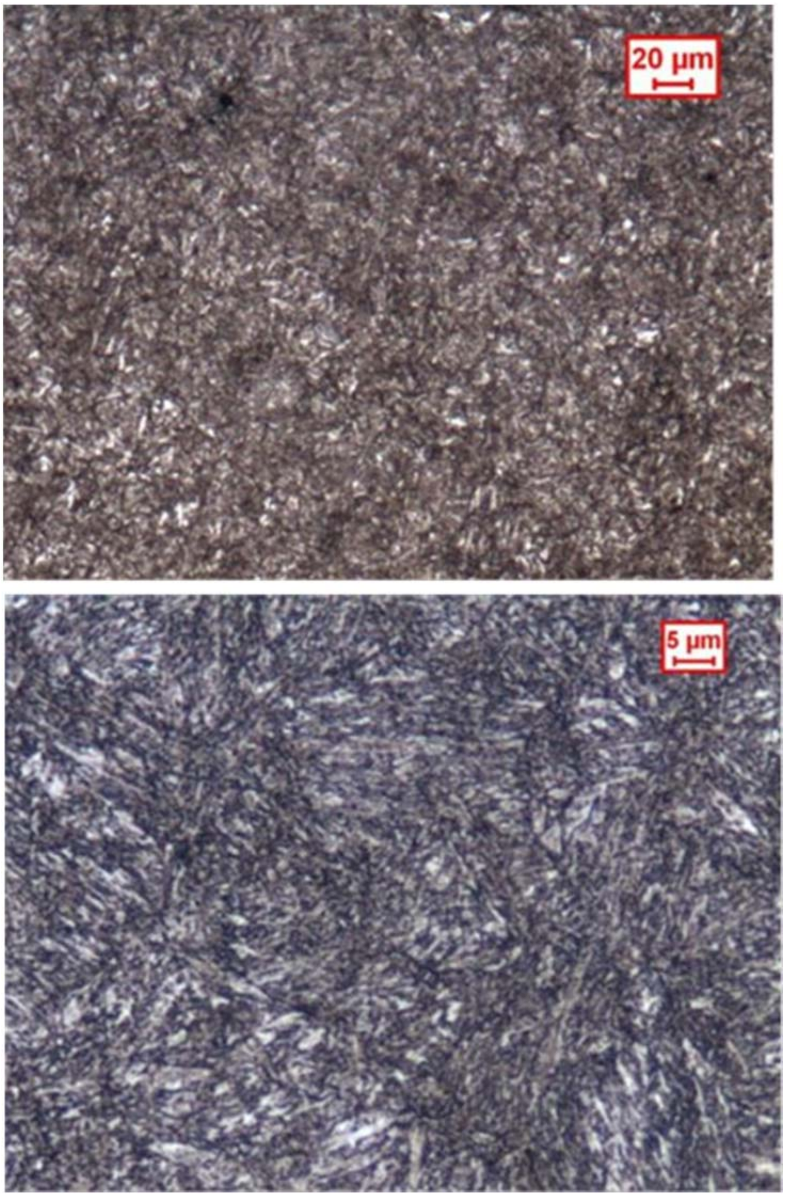

Figure 1: Microstructure of the specimens at different magnification values.

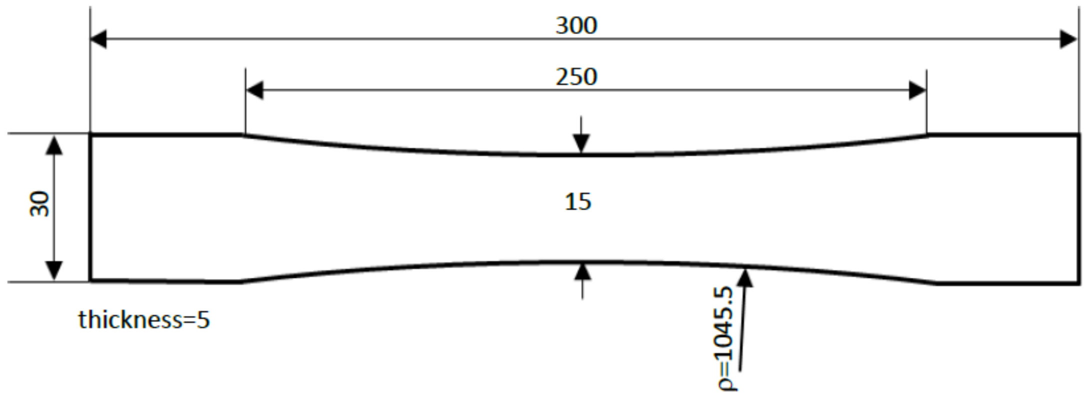

Figure 2: Hour-glass shaped specimen geometry, dimensions in mm.

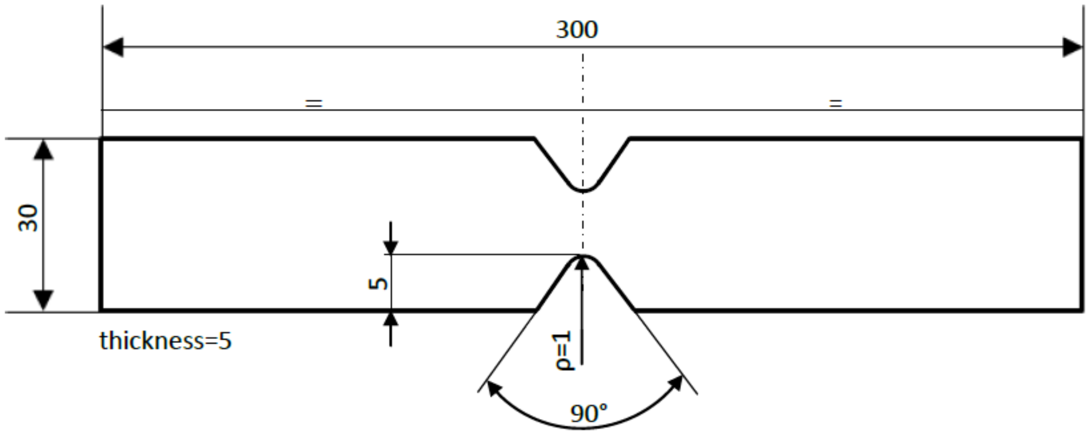

Figure 3: Notched specimen geometry, dimensions in mm.

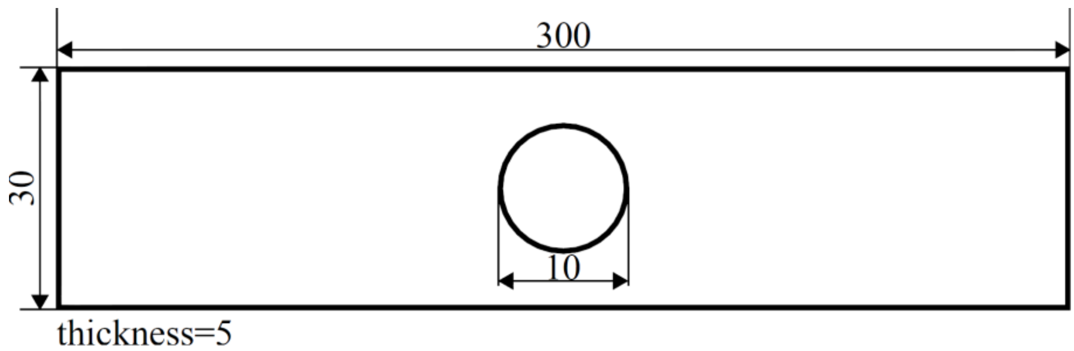

Figure 4: Plates with central hole, dimensions in mm.

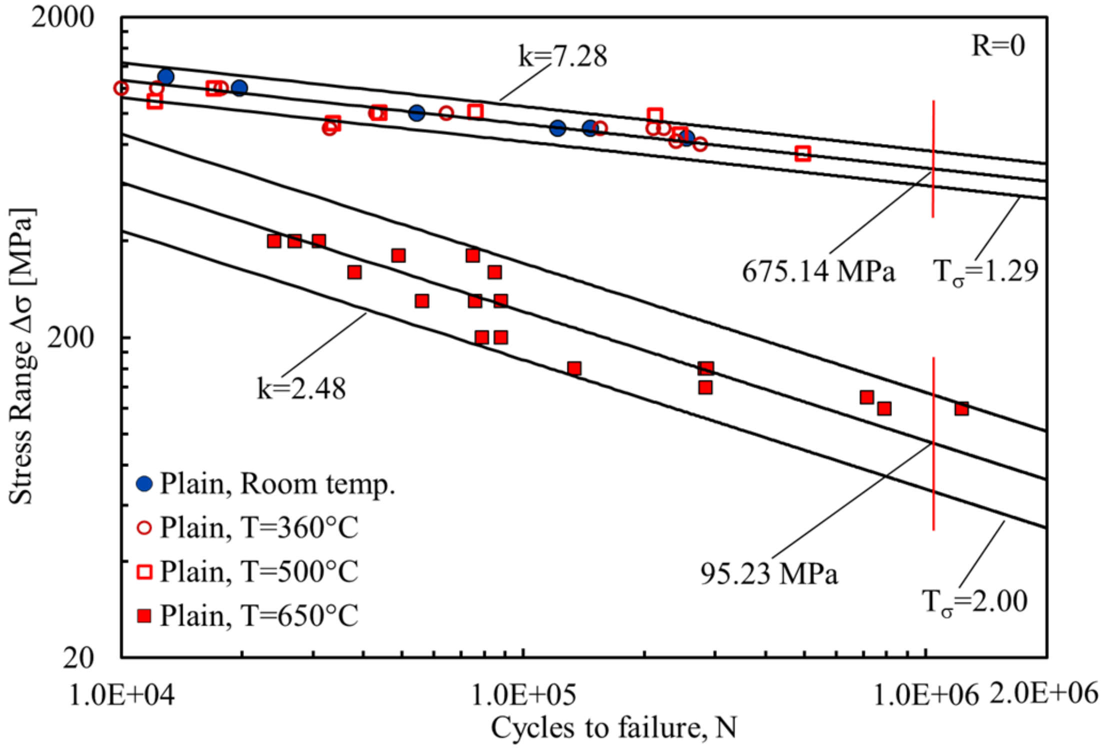

Figure 5: Data from hourglass shaped specimens at different temperatures.

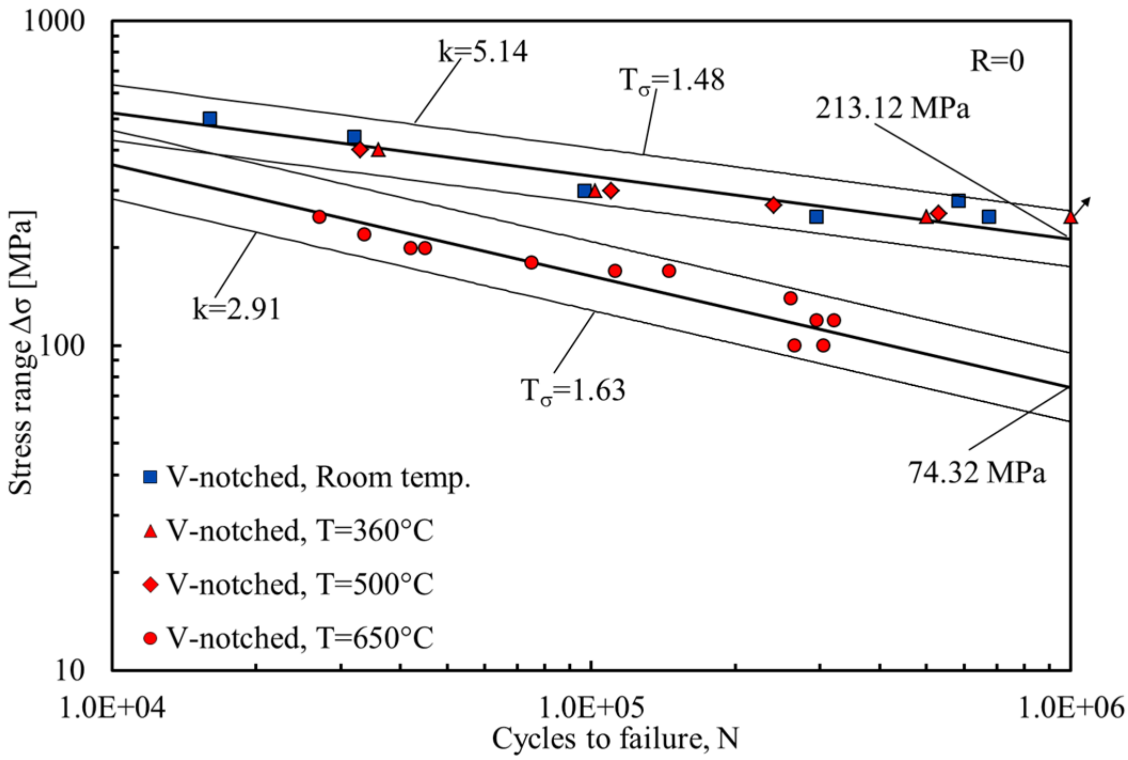

Figure 6: Data from V-notched specimens at different temperatures.

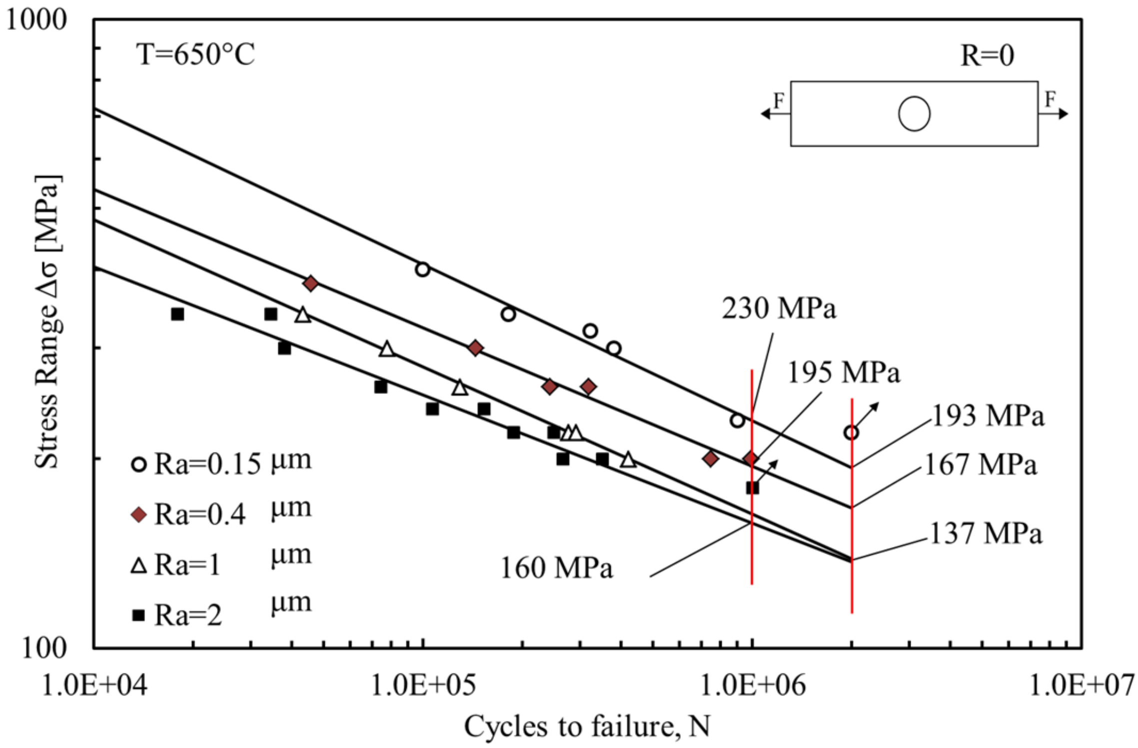

Figure 7: Data from plate with central hole at 650°C, varying the surface roughness.

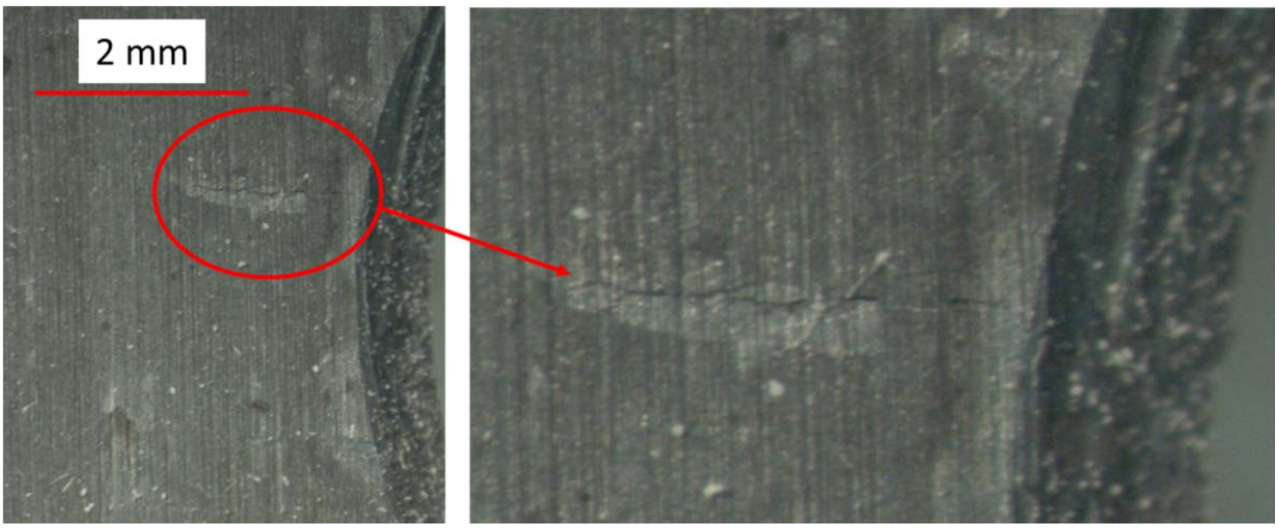

Figure 8: Visual crack detection through optical microscope.

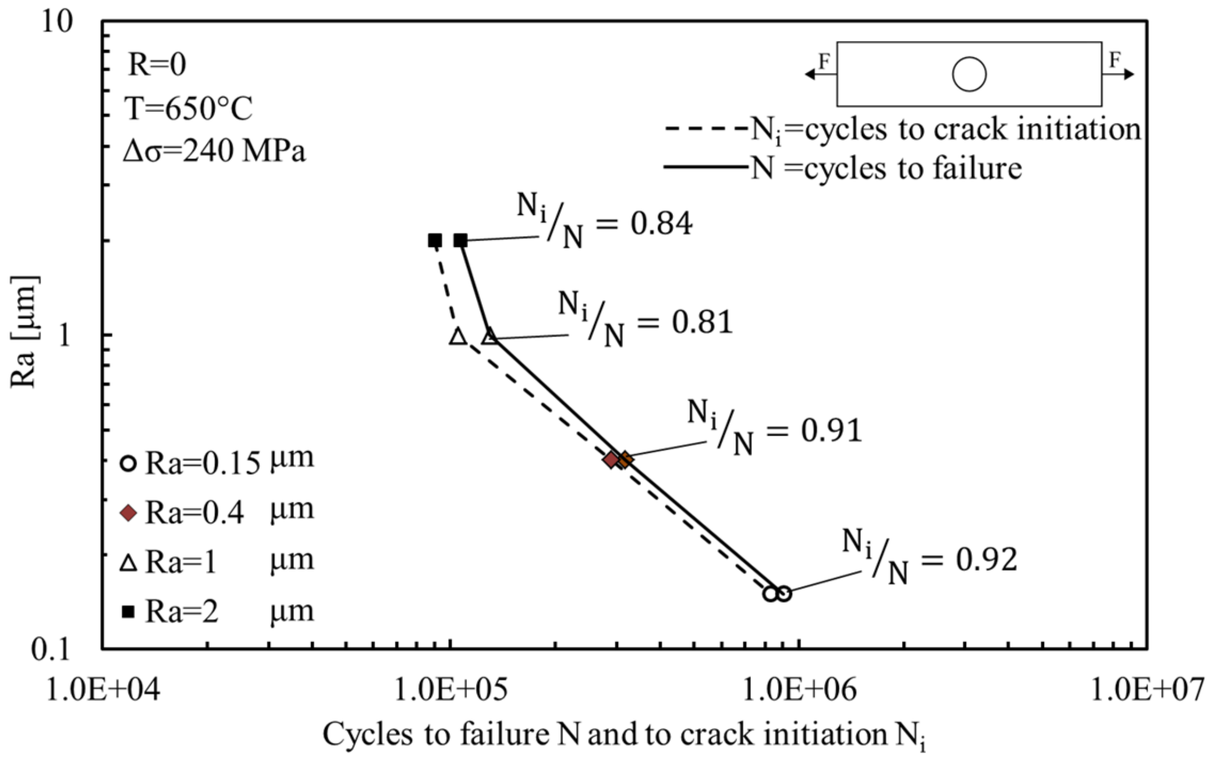

Figure 9: Number of cycles to failure N and for crack initiation N_i for plate with central hole, as a function of the surface roughness.

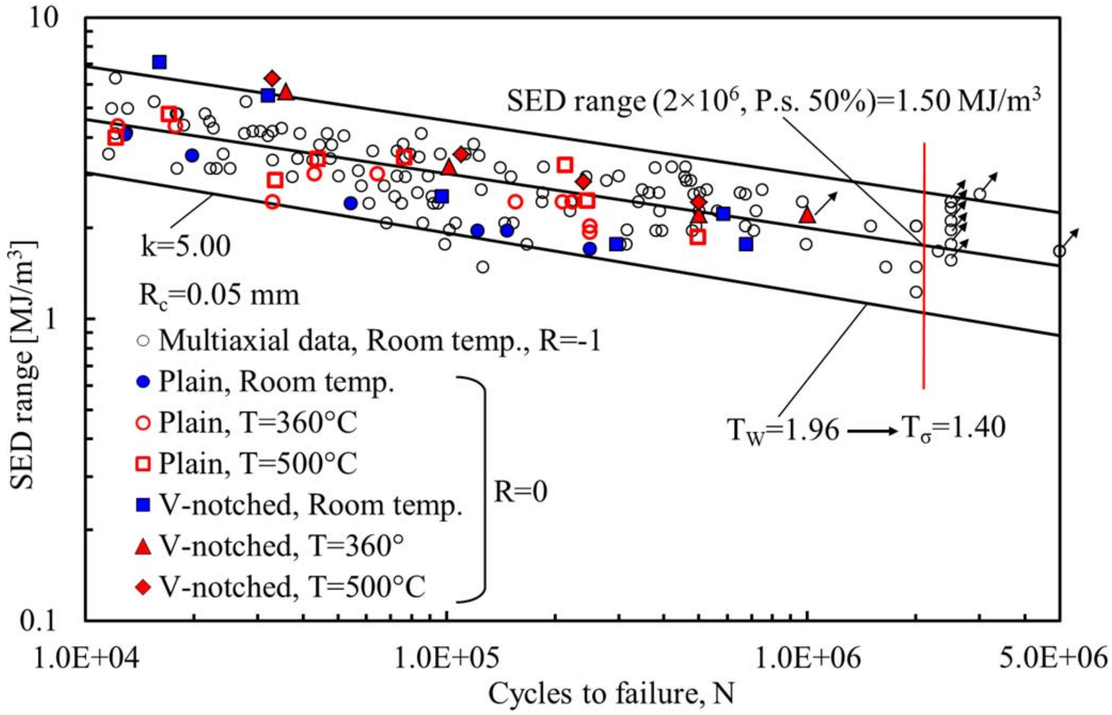

Figure 10: Synthesis by means of local SED of new fatigue data up to 500°C and room temperature multiaxial fatigue data taken from [16].

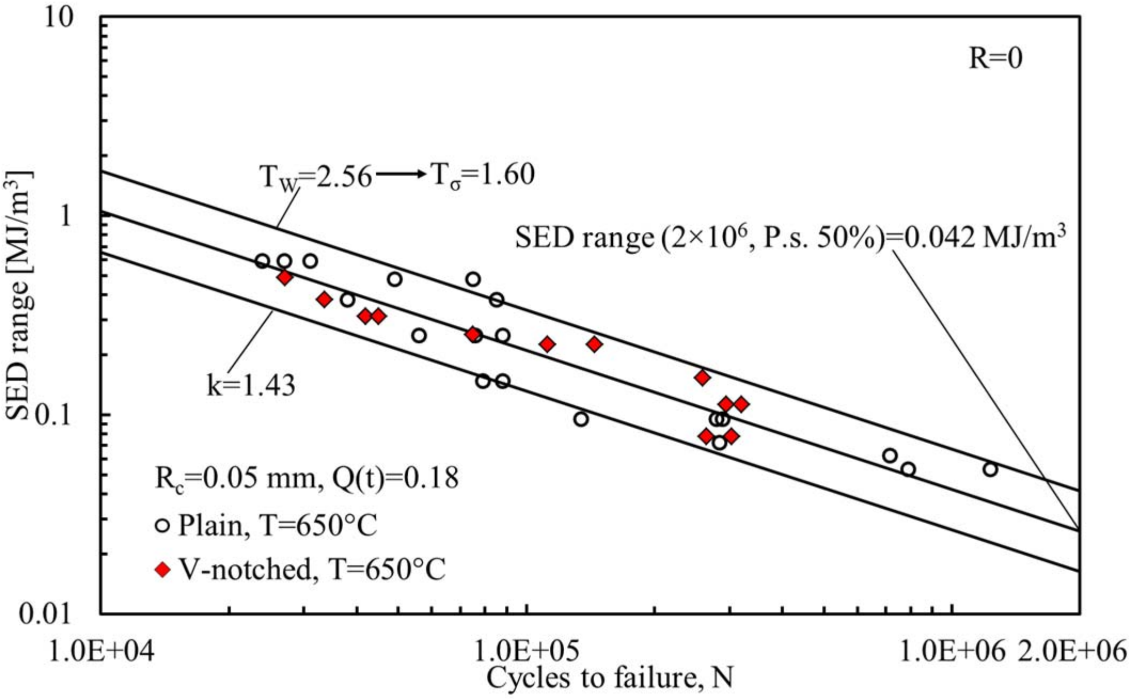

Figure 11: Synthesis by means of local SED of new fatigue data at 650°C of plain and V-notched specimens.